Int. J. Electrochem. Sci., 15 **(2020)** 4592 – 4601, doi: 10.20964/2020.05.48

International Journal of
ELECTROCHEMICAL
SCIENCE
www.electrochemsci.org

Effect of CO_3^{2-} Concentration on the Corrosion Behavior of X80 Pipeline Steel in Simulated Soil Solution

Qiu Li Zhang, Meng Han Xue, Dan Wang, Yang Zi, Jun Zhou[*]

School of Chemistry and Chemical Engineering, Xi'an University of Architecture and Technology, Xi'an, China
[*]E-mail: xazhoujun@126.com

Received: 27 December 2019 / *Accepted:* 11 February 2020 / *Published:* 10 April 2020

In this paper, the effect of CO_3^{2-}concentration on the corrosion behavior of pipeline steels was studied by using potentiodynamic polarization and electrochemical impedance methods in a high-pH simulated soil solution. The results showed that the corrosion of X80 pipeline steel in a Na_2CO_3 solution involved a self-passivation mechanism. As the CO_3^{2-}concentration increased, the protective performance of the passivated film increased, whereas the corrosion rate decreased. When 1 mol/L $NaHCO_3$ was added, the corrosion followed an active-passive mechanism and displayed two anodic peaks. Moreover, the influence of the CO_3^{2-}concentration was different from that of $NaHCO_3$, the $NaHCO_3$ addition increased the corrosion current density, which consequently increased the corrosion rate.

Keywords: pipeline; high-pH simulated solution; potentiodynamic polarization; electrochemical corrosion

1. INTRODUCTION

A large number of pipeline steels, with large diameters and demonstrating high strength and toughness, have been used in oil and natural gas transportation engineering. The transport distance is long and covers a wide area; it even spreads into the complex soil environment. The soil contains a variety of organic matter, inorganic ions, and some bacteria, such as sulfate-reducing bacteria and organic matter degradation-derived CO_2 gas. The organic matter degradation-derived CO_2 gas, which is dissolved in the soil solution, forms corresponding carbonates. The sulfate-reducing bacteria causes the production of H_2S and SO_4^{2-} plasma, which alters the characteristics of the soil and causes the corrosion of pipeline steel. The simulated soil used in studies on soil corrosion is commonly acidic, neutral, and nearly alkaline [1]. Areas in China with acidic soil include Jiangxi Yingtan, whose soil is mainly composed of $CaCl_2$, NaCl, Na_2SO_4, and $MgSO_4 \cdot 7H_2O$ [2]. In contrast, areas with alkaline soil include Korla, Inner Mongolia, and Dagang ancient sand, and the main soil components in these areas include

NaCl, KNO_3, Na_2SO_4, $NaHCO_3$, $MgCl_2·6H_2O$ and $CaCl_2$ [3]. The number of studies on the electrochemical corrosion behaviour of X70 pipeline steel in soil has increased. Y.M. Zeng and J.L. Luo investigated the effect of Cl^- on the local corrosion of X70 pipeline steel in 0.5 mol/L $NaHCO_3$ solution and found that the pitting potential decreased gradually with increasing Cl^- concentration in solution [4]. In addition, L. Zhang et al. simulated Korla alkaline soil and studied the effects of temperature, dissolved oxygen, and pH on the corrosion behaviour of X70 pipeline steel, and they found that dissolved oxygen was the main factor affecting the corrosion behaviour; moreover, low corrosion occurred at a low temperature and with low amounts of dissolved oxygen and weak acid [5]. Gallant et al. reported that the anodic dissolution and passivation transformation of metallic cobalt presented complex electrochemical phenomena in $H_2CO_3/HCO_3^-/CO_3^{2-}$solutions [6]. Eliyan et al. also showed that the corrosion effect of HCO_3^- on steel is complex, and the corrosion mechanism is not clear [7].

With the development of pipeline steels, the application of high-grade pipeline steels has gradually become extensive. X80 pipeline steel has been developed successfully and has been applied to a second line of the approximately 4895 km West Gas Pipeline Project in China [8-9]. Studying the corrosion mechanism of alkali soil to prevent corrosion is highly important. This study investigated the effect of CO_3^{2-} on the corrosion behaviour of X80 pipeline steel in a high-pH soil solution. The electrochemical corrosion mechanism of X80 steel in alkaline soil provides a basis for the modification and application of X80 steel.

2. EXPERIMENT

In this study, the working electrode material was X80 pipeline steel, and the elemental composition is shown in Table 1.

Table 1. Chemical composition of pipeline steel (wt. %)

Element	C	Si	Mn	P	S	Cu	Cr	Ni	Mo	Nb	Ti	V
wt.%	0.04	0.20	1.873	0.009	0.002	0.14	0.25	0.20	0.10	0.055	0.015	0.001

Along the rolled direction X80 pipeline steel was sampled with dimensions of 10 mm(L)×10 mm(W)×2 mm(H). One end was welded to a copper wire using epoxy resin encapsulation, which left a work area of $1cm^2$ that could be used as an electrode. The working face was sequentially polished using #240 to #1500 sandpaper and cleaned with acetone and deionized water. Then it was cleaned, with anhydrous ethanol, blown dry with cold air and placed in a drying box.

The simulated soil solution at a high pH value（pH 9-11）was comprised of $NaHCO_3$ (1.0 mol/L) and Na_2CO_3 (0.5 mol/L) prepared with ACS grade reagents in ultrapure water.

Electrochemical measurements were conducted using a traditional three-electrode system (X80 pipeline steel as a working electrode, high-purity graphite with a large surface area as an auxiliary electrode, and a saturated calomel electrode (SCE) as a reference electrode) on a CS350 electrochemical workstation from Wuhan Correst Company. Unless noted otherwise all potentials were recorded versus SCE. The prepared electrodes were placed in the three-electrode test device followed by pouring in the

corresponding simulation solution. Before the measurement, the working electrode was pre-polarized at -1.2 V for 5 min to remove the oxide film that formed in air and then soaked in the simulation solution for 30 min until the system was stable for the open circuit potential measurement. AC impedance spectroscopy under the open circuit potential was measured for 0.5 h under the following conditions (testing frequency: 100 kHz to 0.01 Hz; disturbance signal amplitude: 5 mV; and, logarithm scanning: 10 times the frequency at 10. Finally, a polarization curve was recorded at a specific parameter setting (potential range: 0.3 ~ 2.0 V_{OCP} (vs. open circuit potential) and scan rate: 0.5 mV/s). Cview analysis software was used for a data fitting analysis of the potentiodynamic polarization curve, as well as ZsimpWin software for the electrochemical impedance spectroscopy test data.

3. RESULTS AND DISCUSSION

As shown in Figure 1, a self-passivation zone occurs when the X80 pipeline steel is in a Na_2CO_3 solution at different concentrations. When the potential is greater than the reduction potential, there is no transition passivation zone, even though the potential is moving. When the passive current density and dimensional passive current density are equal, the steel enters directly into a stable passivation zone. As the concentration of Na_2CO_3 increases, the passive current density and dimensional passive current density decrease, the X80 pipeline steel is more prone to passivation and the passive protection properties of the film are better. The dynamic polarization curves were fitted, and the fitting results are shown in Table 2. In Table 2, B_a indicates the anodic Tafel slope, B_c indicates the cathodic Tafel slope, E_{corr} stands for the corrosion potential and I_{corr} stands for the corrosion current density.

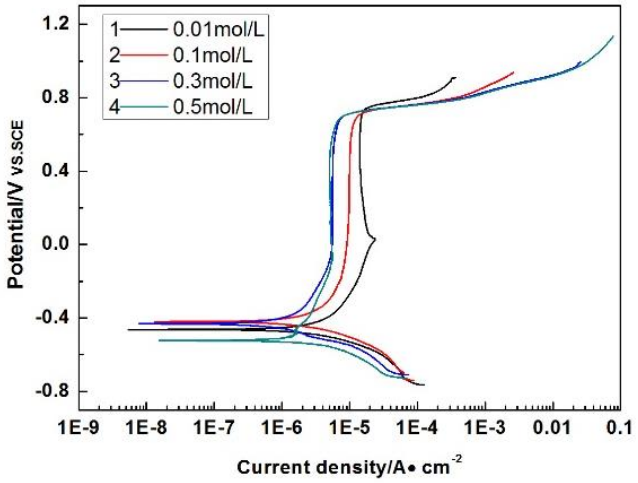

Figure 1. Potentiodynamic polarization curves of the X80 pipeline steel in the Na_2CO_3 aqueous solution at different concentrations

Table 2 shows that along with the increasing concentration of Na_2CO_3, the corrosion current density decreases, the corrosion rate decreases, and its value changes from 0.049 to 0.029. This could be explained by the following. As the concentration of Na_2CO_3 increased, the passivation film was easy to generate on the X80 pipeline steel electrode surface, thereby inhibiting further corrosion.

Figure 2 shows the impedance spectroscopy of the X80 pipeline steel in different concentrations of the Na_2CO_3 solution. Its impedance spectroscopy result was a single capacitive loop, and as the concentration increased, the capacitive reactance arc radius increased additionally, there was a certain diffusion effect in the low frequency region.

Table 2. Potentiodynamic polarization curve fitting values of the X80 pipeline steel in different concentrations of CO_3^{2-}

Na_2CO_3(mol/L)	B_a(mV)	B_c(mV)	E_{corr}(V)	I_{corr}(A/cm^2)	Corrosion Rate(mm/a)
0.01	519	-164	-0.463	4.20×10^{-6}	0.049
0.1	480	-155	-0.419	2.77×10^{-6}	0.033
0.3	606	-151	-0.428	2.60×10^{-6}	0.031
0.5	1258	-135	-0.511	2.53×10^{-6}	0.029

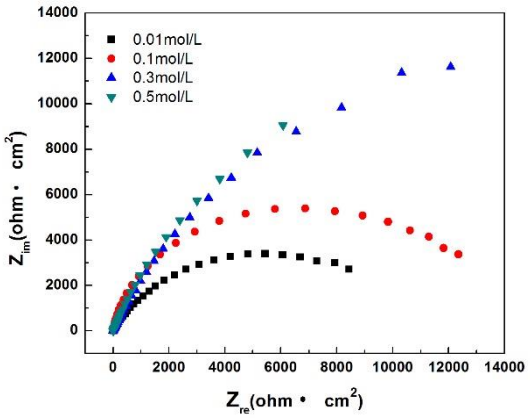

Figure 2. AC impedance spectroscopy of the X80 pipeline steel in different concentrations of the Na_2CO_3 solution

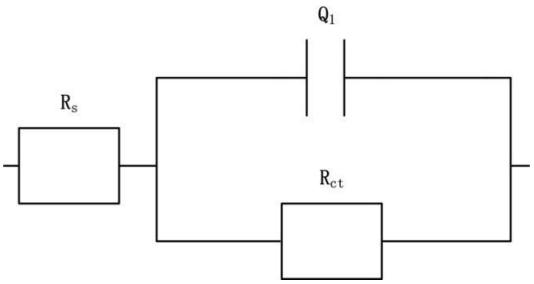

Figure 3. The Equivalent circuit for the AC impedance spectroscopy results of X80 pipeline steel in different concentrations of CO_3^{2-} concentration solution

The size of the capacitive reactance arc represents the resistance of the electrochemical reaction. The larger the capacitive reactance arc is, the greater the electrochemical resistance, and thus, the better its corrosion resistance. The equivalent circuit in Figure 3 R (QR) used for fitting, and the results are shown in Table 3. Rs represents the solution resistance; Q_1 is regular phase angle element, which is different from Cdl because the electrode surface is rough and energy dissipation causes its impedance

spectrum performance to be similar to a constant phase angle element instead of an electric double layer capacitance Cdl; R_{ct} stands for the electrochemical process transfer resistance.

Table 3. Fitting results of the AC impedance spectroscopy of X80 pipeline steel in different concentrations of Na_2CO_3

Na_2CO_3(mol/L)	R_s(ohm·cm2)	Q_1(S·sec^n/cm^2)	R_{ct}(ohm·cm^2)
0.01	29.25	2.74×10^{-4}	9756
0.1	5.46	1.21×10^{-4}	12721
0.3	1.10	3.51×10^{-4}	29225
0.5	1.98	7.81×10^{-4}	36647

Table 3 shows that as the concentration of Na_2CO_3 increases, Rct dramatically increases, indicating that the electrochemical process and mass transfer resistance increase in the Na_2CO_3 solution. Additionally, the ion diffusion increases the resistance of the metal matrix due to the passivation film that covers the surface of the steel; thus, the corrosion rate decreases. In conclusion, as the concentration of Na_2CO_3 increases, the corrosion rate of the X80 pipeline steel decreases, and the effective protection of the passivation membrane increase.

The passivity of the metal surface depends not only on the properties of the metal anode but also on the cathodic oxidation process, which is controlled by the medium. To better explain the corrosion mechanism of X80 pipeline steel in the Na_2CO_3 solution system, one of the curves from Figure 1 is selected as a typical dynamic polarization curve and is shown in Figure 4.

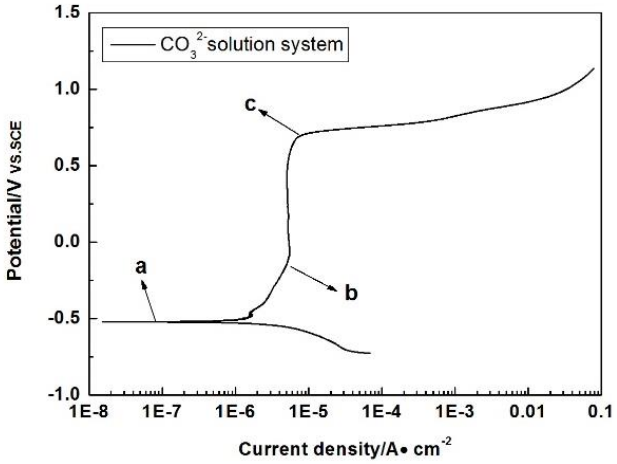

Figure 4. Typical potentiodynamic polarization curves of X80 pipeline steel in the Na_2CO_3 solution

From Figure 4, the electrode surface exhibits stable passivation. The ab segment represents the active dissolution zone of X80 pipeline steel. Within this range, active anode dissolution of the X80 pipeline steel occurs, and the current density increases with increasing electrode potential. Point b is the reduction point of X80 pipeline steel in the Na_2CO_3 solution system. There is no passive presence of a

transition zone, and there is direct access to a stable passive region. The bc segment is a stable passivation region of X80 pipeline steel, corresponding to a current density called the dimensional passive current density. After point C, the steel enters the passivation area. The passivation film is dissolved, which easily induces pitting. In the activation stage, active dissolution of the X80 pipeline steel occurs, which generates Fe^{2+}. The Fe^{2+}combines with OH^-, which is adsorbed on the steel surface to produce unstable Fe $(OH)_2$. Furthermore, there is CO_3^{2-} that easily produces a $FeCO_3$ passivation film on the electrode surface when the product of $[Fe^{2+}] \times [CO_3^{2-}]$ exceeds the solubility, K_{sp}, of $FeCO_3$ [10]. This passivation film layer attaches to the surface of the electrode and further slows the dissolution of the Fe metal. At a high pH, the produced $FeCO_3$ may be further converted into Fe $(OH)_2$ or Fe $(OH)_3$, which attaches to the steel surface [11].

The following reactions may occur and are denoted as specific formula (1)- (4).

Anodic reaction:

$$2Fe \rightarrow 2Fe^{2+} + 4e \quad (1)$$

$$Fe^{2+} + 2OH^- \rightarrow Fe(OH)_2 \quad (2)$$

$$Fe^{2+} + CO_3^{2-} \rightarrow FeCO_3 \quad (3)$$

Cathodic reaction:

$$O_2 + H_2O + 4e^- \rightarrow 4OH^- \quad (4)$$

When 1 mol/L $NaHCO_3$ is added to the solution, the open circuit potentials of the X80 pipeline steel in different concentrations of Na_2CO_3 solution are shown in Figure 5.

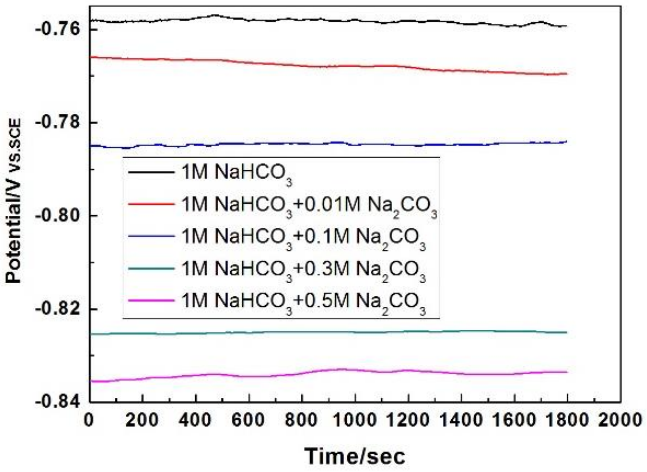

Figure 5. Open circuit potentials of the X80 pipeline steel with different concentrations of Na_2CO_3 containing 1 mol/L $NaHCO_3$

As the concentration increases, the open circuit potential decreases gradually, and when the concentration of Na_2CO_3 increases from 0.1 mol/L to 0.3 mol/L, the open circuit potential decreases by 40 mV, which indicates that an increase in the Na_2CO_3 concentration can increase the surface activity of the electrode. Figure 6 shows the polarization curve of the dynamic potential.

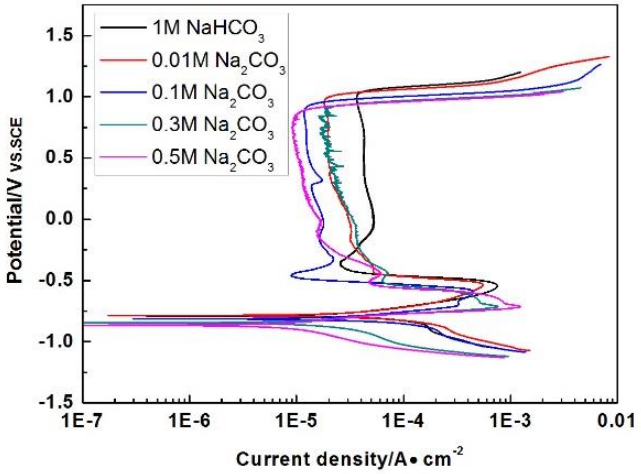

Figure 6. Potentiodynamic polarization curves of the X80 pipeline steel with different concentrations of Na_2CO_3 containing 1 mol/L $NaHCO_3$

As shown in Figure 6, when the solution contains 1 mol/L $NaHCO_3$, its transition passivation zone shows an anodic peak. After adding Na_2CO_3, its transition passivation region displays two anodic peaks, which shows that the introduction of Na_2CO_3 can cause the occurrence of a secondary anodic peak and that the passive film generated by the reaction process changes. At the same time, the concentration of Na_2CO_3 affects the polarization of the first anodic peak potential, namely, the change in magnitude of the reduction potential. When the concentration of Na_2CO_3 is less than 0.01 mol/L, its critical passive potential is approximately 0.543V; when the concentration is 0.1 mol/L, the value is 0.593 V. Furthermore, when the concentration is greater than 0.3 mol/L, the critical passive potential is 0.713 V. Thus, with increasing concentration, the critical passive potential decreases, which has been previously mentioned in this paper. The first anodic peak corresponds to the formation of the $FeCO_3$ passivation membrane; therefore, the Na_2CO_3 concentration increases and the formation of the $FeCO_3$ passivation film occurs. The Na_2CO_3 concentration may also affect the passivation potential (Etr) of X80 pipeline steel in the solution. With increasing Na_2CO_3 concentration, the passivation potentials are 1.018 V, 0.984 V, 0.914 V, 0.901 V and 0.862 V. Thus, the reduction potential is reduced, and the passivation membrane is stable. The increase in Na_2CO_3 concentration also leads to decrease in the dimensional passive current density, and as a result, Na_2CO_3 can increase the effective protection that comes from the passivation film. The fitting results of the polarization curve are shown in Table 4.

Table 4. The Fitting results of the potentiodynamic polarization curve in Figure 6

Na_2CO_3(mol/L)	B_a(mV)	B_c(mV)	E_{corr}(V)	I_{corr}(A/cm^2)	Corrosion Rate(mm/a)
0	175	-134	-0.790	5.18×10^{-5}	0.609
0.01	179	-137	-0.786	4.92×10^{-5}	0.578
0.1	88	-60	-0.814	2.29×10^{-5}	0.270
0.3	79	-83	-0.846	8.23×10^{-6}	0.099
0.5	74	-133	-0.866	5.17×10^{-6}	0.060

From Table 4, it can be seen that when the CO_3^{2-}concentration in the HCO_3^--CO_3^{2-} solution is 0 mol/L, the corrosion rate of X80 steel is the largest, and its value is 0.609 mm/a. The concentration of Na_2CO_3 increases with the decrease in E_{corr} and the corrosion rate, and the corrosion activity of the electrode surface is low. When the CO_3^{2-}concentration reaches 0.5 mol/L, the corrosion rate reaches 0.060 mm/a. Therefore, it is not easy for corrosion to occur in the presence of a high CO_3^{2-} concentration when the HCO_3^-concentration in the HCO_3^--CO_3^{2-} solution is constant. The above observation indicates that the surface of the electrode easily forms a passivation film, which can slow down the reaction of the metal matrix and corrosive medium further and reduce the corrosion rate of X80 pipeline steel. The comparison of Table 2 and Table 4 shows that although the corrosion rate after adding $NaHCO_3$ is greater than that without adding $NaHCO_3$, the corrosion rate still shows a downward trend. According to the research conclusion of Eliyan et al. [12], the concentration of HCO_3^- can increase the corrosion rate of API-X100 pipeline steel in a CO_2 solution, which is consistent with the results of this work. When the CO_3^{2-}concentration changes from 0 mol/L to 0.5 mol/L, the corrosion rate decreases by 39%, as shown in Figure 2, and decreases by 90%, as shown in Figure 4. At a high pH, the HCO_3^- concentration has a certain effect on the corrosion rate [13]. HCO_3^- is mainly a reduction reaction, which increases the coverage of OH^- on the steel surface and promotes the formation of corrosion product films [14-15]. The OH^- consumed by the reaction will promote the hydrolysis of CO_3^{2-}, which will provide more OH^- and reduce the corrosion rate. On the one hand the first corrosion film may contain $Fe(OH)_2$ intermediates and $FeCO_3$ crystals, and the stability and density of the film are not sufficient [16]; on the other hand, the presence of oxygen in the solution will accelerate the further oxidation of $FeCO_3$ [17-18]. Therefore, the initial corrosion film is easily broken or dissolved. Even if this happens, because the OH^- in the solution is very small in size, it will quickly enter the defect point to restart the reaction. At the same time, at a high pH, solid $FeCO_3$ will be formed on the surface of the steel, which will cause secondary passivation. A dense corrosion product film can reduce the contact between the material matrix and the corrosive medium, which reduces the corrosion rate [19].

Figure 7 shows the impedance spectroscopy of X80 pipeline steel in different concentrations of Na_2CO_3 which contains 1 mol/L $NaHCO_3$.

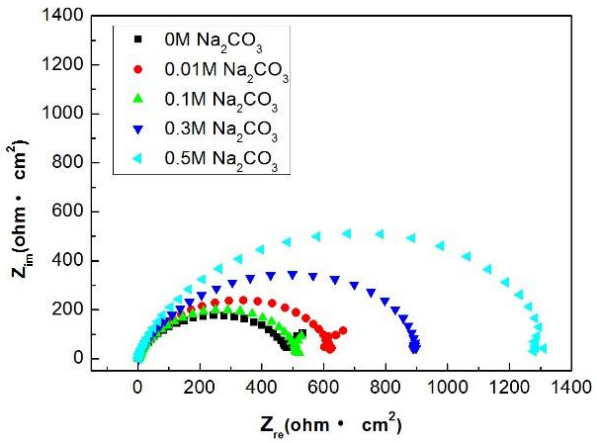

Figure 7. Impedance spectroscopy of the X80 pipeline steel in different concentrations of Na_2CO_3 containing 1mol/L $NaHCO_3$

It can be seen from the diagram that under the condition of the open circuit potential, the AC impedance spectroscopy is a flat half arc, and as the concentration increases, the radius in the low frequency area increases. The equivalent circuit shown in Figure 3 R (QR) is used to obtain the fitting, and the fitting results are shown in Table 5.

Table 5. Fitting values of the AC impedance spectrum in Figure 7

Na_2CO_3(mol/L)	R_s(ohm·cm^2)	Q_1(S·sec^n/cm^2)	R_{ct}(ohm·cm^2)
0	2.80	3.61	502.1
0.01	1.89	2.48×10^{-4}	617.8
0.1	1.90	2.84×10^{-4}	510.2
0.3	2.59	3.39×10^{-4}	915.6
0.5	2.49	2.98×10^{-4}	1315

As seen from Table 5, when the solution contains 1 mol/L $NaHCO_3$, along with Na_2CO_3, the overall trend of R_{ct} increases; that is, the charge transfer resistance increases, and the corrosion rate decreases. All of which are consistent with the results of the polarization curve analysis.

4. CONCLUSION

The mechanism of corrosion of X80 pipeline steel in a Na_2CO_3 solution was a self-passivation process. As the CO_3^{2-} concentration increases, the passive current density and the dimensional passive current density decrease, while the protective property of the passivation membrane is enhanced. The higher the CO_3^{2-} concentration is, the larger the resistance R_{ct}, which both result in the corrosion rate decreasing when the concentration of CO_3^{2-} increases. When a $NaHCO_3$ solution (1 mol/L) is added, the corrosion process shows an activation-passivation mechanism with the presence of two anodic peaks. The influence of the CO_3^{2-} concentration with and without $NaHCO_3$ are the same. A comparison shows that the addition of $NaHCO_3$ can increase the corrosion current density, reduce the charge transfer resistance, and increase the corrosion rate.

ACKNOWLEDGEMENTS
The authors acknowledge the Natural Science Basic Research Plan in Shaanxi Province of China (Program No.2018JM5138).

References

1. Q. Wang, Z.Q. Bai, J. Miao, B. Wei, L. Y. Geng and G. Li, *Corros.Sci. Prot. Technol.*,24(2012)

171.
2. C. Li, C.W. Du, Z.Y. Liu and X.G. Li, *Corros.Sci. Prot. Technol.*, 24(2012)327.
3. J. Xiao, *Study on the SCC behaviors of X80 pipeline steels in Korla soil simulated solution*, LiaoNing Shiyou University,2010, LiaoNing, China.
4. Y.M. Zeng, J.L. Luo and P.R. Norton, *Electrochim. Acta*, 49(2004)703.
5. L. Zhang, X.G. Li and C.W. Du, *J. Iron. Steel Res. Int.*, 16(2009)52.
6. D. Gallant, M. Pézolet, A. Jacques and S. Simard, *Corros.Sci.*,48(2006)2547.
7. F.F. Eliyan and A. Alfantazi, *Corrosion*,70(2014)880.
8. W. Zhou, W. Lan, X. L. Cao, H. D. Deng, Y. B. Yan, X. L. Hou, *Int. J. Electrochem. Sci.*, 13 (2018) 1283.
9. S.X. Wu, Z.M. Gao, J. Zhao, L.Q. Wang, Y.J. Liu, M.J. Wu and W.B. Hu, *Int. J. Electrochem. Sci.*, 15 (2020) 868
10. H.W. Liu, T.Y. Gu, G.A. Zhang, H.F. Liu and Y. Frank Cheng, *Corros.Sci.*,136(2018)47.
11. R.F. Wright, E. R. Brand, M. Z. Moroz, J. H. Tylczak and P. R. Ohodnicki Jr, *Electrochim. Acta*,290(2018)626.
12. F. F. Eliyan and A. Alfantazi, Mater. *Chem.Phys.*,140(2013)508.
13. J. Han, J. Zhang and J. W. Carey, *Int. J. Greenh. Gas Contr.*, 5(2011)1680.
14. M. Nordsveen, S. Nesic, R. Nyborg and A. Stangeland, *Corrosion* ,59(2003)443.
15. A. Wiecknowski, E. Ghali, M. Szklarczyk and J. Sobkowski, *Electrochimi. Acta*,28(1983)1619.
16. Y.B. Yan, H.D. Deng, W.W. Xiao, T.X. Ou and X.L. Cao, *Int. J. Electrochem. Sci.*, 15 (2020) 1713.
17. P. Refait, M. Jeannin, R. Sabot, H. Antony and S. Pineau, *Corros. Sci.*, 90 (2015) 375.
18. X. Wang, X.Y. Wang, J. Wang, G.W. Wang, Y. Pan and S.C. Yan, *Int. J. Electrochem. Sci.*, 15 (2020) 889.
19. G.W. Li, B.S. Huang, S.S. Zhang, X. Wen and T.N. Li, *Int. J. Electrochem. Sci.*,15(2020)121.